

Participation of the surface structure of *pharaonis* phoborhodopsin, ppR and its A149S and A149V mutants, consisting of the C-terminal  $\alpha$ -helix and E-F loop, in the complex-formation with the cognate transducer pHtrII, as revealed by site-directed  $^{13}\text{C}$  solid-state NMR

Izuru Kawamura,<sup>1</sup> Yoichi Ikeda,<sup>2</sup> Yuki Sudo,<sup>2</sup> Masayuki Iwamoto,<sup>2</sup> Kazumi Shimono,<sup>2</sup> Satoru Yamaguchi,<sup>3</sup> Satoru Tuzi,<sup>3</sup> Hazime Saitô,<sup>3,4</sup> Naoki Kamo<sup>2</sup> and Akira Naito<sup>1\*</sup>

<sup>1</sup>Graduate School of Engineering, Yokohama National University, 79-5 Tokiwadai, Hodogaya-ku, Yokohama, Japan 240-8501, <sup>2</sup>Laboratory of Biophysical Chemistry, Graduate School of Pharmaceutical Sciences, Hokkaido University, Sapporo, Japan 060-0812, <sup>3</sup>Department of Life Science, Himeji Institute of Technology, University of Hyogo, Harima Science Garden City, Kamigori, Hyogo, Japan 678-1297 and <sup>4</sup>Center for Quantum Life Sciences, Hiroshima University, Kagamiyama, Higashi-Hiroshima, Japan 739-8526

\*Corresponding Author: A. Naito

E-mail: [naito@ynu.ac.jp](mailto:naito@ynu.ac.jp)

## ABSTRACT

We have recorded  $^{13}\text{C}$  solid state NMR spectra of  $[3\text{-}^{13}\text{C}]\text{Ala}$ -labeled *pharaonis* phoborhodopsin *ppR*, and its mutants, A149S and A149V, complexed with the cognate transducer *pHtrII* (1-159), to gain insight into a possible role of their cytoplasmic surface structure including the C-terminal  $\alpha$ -helix and E-F loop for stabilization of the 2:2 complex, by both cross-polarization magic angle spinning (CP-MAS) and dipolar decoupled-magic angle spinning (DD-MAS) NMR techniques. We found that  $^{13}\text{C}$  CP-MAS NMR spectra of  $[3\text{-}^{13}\text{C}]\text{Ala}$ -*ppR*, A149S, and A149V complexed with the transducer *pHtrII* are very similar, reflecting their conformation and dynamics changes caused by mutual interactions through the transmembrane  $\alpha$ -helical surfaces. In contrast, their DD-MAS NMR spectral features are quite different between  $[3\text{-}^{13}\text{C}]\text{Ala}$ - A149S and A149V in the complexes with *pHtrII*:  $^{13}\text{C}$  DD-MAS NMR spectrum of  $[3\text{-}^{13}\text{C}]\text{Ala}$ -A149S complex is rather similar to that of the uncomplexed form, while the corresponding spectral feature of A149V complex is similar to that of *ppR* complex in the C-terminal tip region. This is because more flexible surface structure detected by the DD-MAS NMR spectra are more directly influenced by the dynamics changes than the CP-MAS NMR. It turned out, therefore, that an altered surface structure of A149S resulted in destabilized complex as viewed from the  $^{13}\text{C}$  NMR spectrum of the surface areas, probably because of modified conformation at the corner of the helix F in addition to the change of hydrophathy. It is, therefore, concluded that the surface structure of *ppR* including the C-terminal  $\alpha$ -helix and the E-F loops is directly involved in the stabilization of the complex through conformational stability of the helix F.

## INTRODUCTION

The archaeal sensory rhodopsins, SRI and SRII, are sensors for positive and negative phototaxis, respectively, on binding with the cognate transducer proteins (1). *Pharaonis* phoborhodopsin (*ppR*) is a negative phototaxis receptor, and forms a complex with *pharaonis* halobacterial transducer II protein (*pHtrII*). The stoichiometry of the *ppR-pHtrII* complex has been estimated to be 2:2 in cell membrane. When blue light is irradiated, this complex activates the phosphorylation cascade in the cytoplasmic side and regulates the switch of flagella motor (2-5).

The *ppR-pHtrII* interactions have been well investigated by using x-ray diffraction (XRD), FTIR spectroscopy, etc: it was shown that the Y199<sup>*ppR*</sup>-N74<sup>*pHtrII*</sup>, and T189<sup>*ppR*</sup>-E43<sup>*pHtrII*</sup> and S62<sup>*pHtrII*</sup> hydrogen bonds are formed between the binding surfaces of *ppR* and *pHtrII* in the transmembrane and extracellular region (6-10). In particular, Tyr199 conserved even in sensory rhodopsin II is a very important residue when *ppR* forms a complex with its cognate *pHtrII* (11,12). In addition, FTIR results strongly indicated that Thr204-Tyr174 forms a hydrogen bond between the retinal pocket and binding surface of *ppR-pHtrII*, and Tyr199 and Thr204 in helix G play an important role for the interaction with *pHtrII* (13-15). On the other hand, the *ppR-pHtrII* interactions in the cytoplasmic regions are very important to take part in a signal relay, because the E-F loop in *ppR* turned out to interact with membrane proximal region in *pHtrII* as viewed from fluorescent probes (16). Further, *pHtrII*(1-114) in the cytoplasmic side is tightly bound with *ppR* inhibiting the proton release, although this activity depends on the length of *pHtrII* (17). It is also reported that the introduction of mutation into membrane proximal region in *HtrI* activates the proton release in SRI in spite of *HtrI* binding with SRI (18).

Fully hydrated membrane proteins are not always rigid solid at ambient temperature but rather flexible, exhibiting a variety of local motions as revealed by site-directed  $^{13}\text{C}$  NMR, which are well related with their biological functions (19-22). Site-specific assignments of individual  $^{13}\text{C}$  NMR peaks recorded by MAS NMR are essential to locate such portions, as demonstrated for the previous  $^{13}\text{C}$  NMR studies on  $[3\text{-}^{13}\text{C}]\text{Ala-}$ ,  $[1\text{-}^{13}\text{C}]\text{Val-}$  and  $[1\text{-}^{13}\text{C}]\text{Trp-}$ labeled bacteriorhodopsin (bR) from purple membrane (23-25). To this end, a variety of approaches such as cleavage of the C-terminal residues, site-directed mutation, and line-broadenings due to  $\text{Mn}^{2+}$  ion-induced transverse relaxation process were utilized. As a result, the organization of the cytoplasmic surface structures, including the C-terminal  $\alpha$ -helix and the E-F loop as a function of metal ions, pH, temperature, etc., plays an essential role for the stabilization of the three-dimensional structure of bR at ambient temperature (26-29). It is demonstrated here that the  $^{13}\text{C}$  NMR signals of the C-terminal  $\alpha$ -helical region were also recently identified for  $[3\text{-}^{13}\text{C}]\text{Ala-}$  and  $[1\text{-}^{13}\text{C}]\text{Val-}$ labeled *ppR* and D75N mutant in the presence or absence of *pHtrII*(1-159) in egg PC bilayers (30-32) (see Figure 1 for the amino-acid sequence of *ppR*).

In this paper, we examined the conformation and dynamics of  $[3\text{-}^{13}\text{C}]\text{Ala-}$ labeled *ppR*, A149S and A149V mutants of *ppR* with emphasis of a possible role of the E-F loop by means of  $^{13}\text{C}$  solid-state NMR techniques with reference to those of bR previously examined (26-28), because Ala149 in *ppR* is highly preserved on the other archaeal retinal proteins (11). The isotropic  $^{13}\text{C}$  CP-MAS NMR peak of Ala149 was initially assigned by comparing  $^{13}\text{C}$  NMR peak of  $[3\text{-}^{13}\text{C}]\text{Ala-}$ labeled *ppR* with that of  $[3\text{-}^{13}\text{C}]\text{Ala-}$ labeled A149S and A149V. We further examined the corresponding spectral changes of  $^{13}\text{C}$  DD-MAS NMR for  $[3\text{-}^{13}\text{C}]\text{Ala-}$ labeled A149S and A149V complexed

with *pHtrII*(1-159). It turned out that mutation of *ppR* at Ala149 resulted in dynamical changes of the *ppR-pHtrII*(1-159) complex as far as membrane surface is concerned. It is therefore suggested that residues in the E-F loop regulate dynamics of membrane surface residues in *ppR* by binding with *pHtrII*.

## **MATERIALS AND METHODS**

[3-<sup>13</sup>C]Ala-, [1-<sup>13</sup>C]Val-labeled A149S and A149V of *ppR* with His-Tag (6 × His) at the C-terminal were expressed in *Escherichia coli* BL21(DE3) strain in M9 medium containing [3-<sup>13</sup>C] L-Alanine and [1-<sup>13</sup>C] L-Valine (CIL, Andover, MA) by induction with 1 mM IPTG and 10 μM all-*trans* retinal. These proteins were solubilized by using n-dodecyl-β-D-maltoside (DM) and purified with a Ni-NTA column (QIAGEN, Hilden, Germany) as described previously (32,33). The truncated transducer, *pHtrII*(1-159), was prepared by using the above method. Purified proteins in DM micelles were incorporated into a lipid film of egg PC (*ppR*: egg PC molar ratio of 1:50), followed by gently stirring at 4 °C for overnight. DM was removed using Bio-Beads (Bio-Rad, Hercules, CA) to yield egg PC bilayers. Reconstituted suspensions were concentrated by centrifugation and suspended in 5 mM HEPES, 10 mM NaCl buffer solution (pH 7). The pelleted mixture of the complex with *ppR*: *pHtrII* ratio of 1:1 in egg PC bilayers was placed in 5.0 mm o.d. zirconia pencil-type rotor for magic angle spinning (MAS) experiments.

High-resolution <sup>13</sup>C solid-state NMR spectra were recorded on a Chemagnetics CMX-400 infinity FT-NMR spectrometer at 100.16 MHz for the carbon resonance frequency. Both cross polarization-magic angle spinning (CP-MAS) and single pulse excitation with dipolar decoupling-magic angle spinning (DD-MAS) were used to

record  $^{13}\text{C}$  NMR spectra. Mostly, 5000 transients were accumulated and 30 Hz of Gaussian broadening function was applied at the center point of 0.40 prior to Fourier transformation. A doubly tuned MAS probe equipped with a 5.0 mm o.d. rotor was used. The spinning frequency was set to 4 kHz and the duration of  $90^\circ$  pulse for the observed  $^{13}\text{C}$  nucleus was 5.5  $\mu\text{s}$ . In CP-MAS experiments, two pulses phase modulation (TPPM) proton decoupling (34) was used, and the contact and repetition times were 1 ms and 4 s, respectively. At ambient temperature, fully hydrated *ppR* undergoes fluctuation motions with frequency range from  $10^2$  to  $10^8$  Hz depending on its location (30). These wide dynamic ranges allowed us to distinctly observe motional components with the frequency range of  $10^6$ - $10^8$  Hz by DD-MAS and rigid components with the frequency range of  $10^2$ - $10^6$  Hz by CP-MAS methods. When the frequency of incoherent random molecular fluctuations in the region with the order of  $10^4$ - $10^5$  Hz could be interfered with frequency of magic angle spinning or proton decoupling frequency, and hence observed  $^{13}\text{C}$  NMR signal in such region could be broadened or suppressed as a low efficiency of peak narrowing (35, 36).  $^{13}\text{C}$  chemical shifts were externally referred to 176.03 ppm for the carbonyl carbon of glycine from TMS.

## RESULTS

### Transmembrane $\alpha$ -helical portion of wild type *ppR* and mutants at Ala149

Figure 2 illustrates the  $^{13}\text{C}$  CP-MAS NMR spectra of  $[3\text{-}^{13}\text{C}]\text{Ala-ppR}$  (A) (30), A149S (B) and A149V (C) reconstituted in egg PC bilayers at ambient temperature. The  $^{13}\text{C}$  NMR peak at 14.1 ppm was assigned to that of the methyl carbon from egg PC (30).

The assignment of the upper field shoulder peak at 14.1 ppm of *ppR* in egg PC is not clear at present, although this peak arises definitely from the portion of lipids and not present in the  $^{13}\text{C}$  NMR spectra of the mutants. It should be noted that many of the  $^{13}\text{C}$  NMR peaks of  $[3\text{-}^{13}\text{C}]\text{Ala-bR}$  were resonated at the peak-position of the  $\alpha_{\text{II}}$ -helix at 15.9-16.9 ppm which is resonated at lower field portion of the conformation-dependent  $^{13}\text{C}$  chemical shift of  $\alpha$ -helical Ala  $\text{C}_\beta$ , in the presence of dynamics-dependent  $^{13}\text{C}$  chemical shifts for  $\alpha$ -helix (19,27), rather than the plausibly distorted torsion angles as proposed by Krimm and Dwivedi based on IR spectra (37). It is noteworthy that the peak-intensity at 15.9 ppm from the  $^{13}\text{C}$  CP-MAS NMR spectra of  $[3\text{-}^{13}\text{C}]\text{Ala-A149S}$  and A149V proteins is significantly reduced with reference to that of  $[3\text{-}^{13}\text{C}]\text{Ala-ppR}$  owing to the absence of the  $^{13}\text{C}$  signals in these mutants (see Figures 2 (A)-(D)). In fact, this is consistent with the difference spectrum between  $[3\text{-}^{13}\text{C}]\text{Ala-ppR}$  and  $[3\text{-}^{13}\text{C}]\text{Ala-A149S}$  (see Figure 2(D)). The reduced peak area is 0.06 out of whole area between 14.5 and 16.9 ppm. This value is twice as large as that of 0.03 as estimated from the number of labeled Ala residues in *ppR*, namely 1/31. This is because a part of Ala  $\text{C}_\beta$  does not appear in the  $^{13}\text{C}$  CP-MAS NMR spectrum. Therefore, the  $^{13}\text{C}$  NMR peak at 15.9 ppm can be uniquely assigned to Ala149 which is involved in the  $\alpha$ -helix portion with reference to the conformation-dependent  $^{13}\text{C}$  chemical shifts of the  $\alpha$ -helix [19, 27, 38]. In particular, Ala149 is located in the  $\alpha_{\text{II}}$ -helix portion near at the E-F loop in the cytoplasmic side, as judged from the conformation-dependent  $^{13}\text{C}$  chemical shifts (19, 27, 389 (Figure 1)).

Figure 3 shows the  $^{13}\text{C}$  CP-MAS NMR spectra of  $[3\text{-}^{13}\text{C}]\text{Ala}$ -labeled *ppR* (A) [30], A149S (B), and A149V (C) which are complexed with *pHtrII*(1-159) in egg PC bilayers. As compared with the spectral patterns in the absence of the transducer (Figure

2A), the five (or six) well-resolved signals were observed for *ppR* and mutants at Ala 149, when they are complexed with *pHtrII*(1-159) (Figure 3). It should be pointed out that the contribution of peaks in the region between 14.5 and 16.9 ppm, from residues of natural abundance in *pHtrII* appeared to be very low. This is because 18Ala C<sub>β</sub>, 15Ile C<sub>γ2</sub>, and 5Met C<sub>ε</sub> are possibly resonated at this region (39) in the vicinity of Ala C<sub>β</sub> but the relative peak intensity from natural abundance is extremely low (less than 1.5%) compared with the <sup>13</sup>C-labeled peaks from 31Ala C<sub>β</sub> of *ppR*. In fact, no such contribution was seen for similar preparations of [3-<sup>13</sup>C]Ala-labeled bR (40). The observed spectral changes in the complex formation mainly from the transmembrane region are obviously explained in terms of the accompanied conformational and dynamics changes due to the presence of van der Waals contact and hydrogen bonds in the binding surface of the transmembrane α-helices between *ppR* and *pHtrII*, since the CP-MAS NMR spectra mainly reflect the changes in the transmembrane regions of the *ppR-pHtrII*(1-159) complex. Naturally, the peak-intensity at 15.8-15.9 ppm in the CP-MAS NMR is significantly reduced in the mutants, because no <sup>13</sup>C NMR signal from Ala 149 is present. The interaction of *pHtrII* with *ppR* increases the thermal stability of *ppR* with the formation of Y199<sup>*ppR*</sup>-N74<sup>*pHtrII*</sup> hydrogen bond in the transmembrane region (14). In fact, it is confirmed that Ala149 mutants interacted with *pHtrII*(1-159) increases the thermal stability (data not shown). These results indicate that the structure and dynamics of the transmembrane region are retained in these mutants in which Y199<sup>*ppR*</sup>-N74<sup>*pHtrII*</sup> hydrogen bond is conserved even in the Ala149 mutants (5,12,13).

### **Membrane surface residues of *ppR* and Ala149 mutants**

It is noteworthy that the peak-intensities of the two kinds of  $^{13}\text{C}$  NMR peaks for  $[3-^{13}\text{C}]\text{Ala}$ -labeled *ppR* and A149V, resonated at 16.7-16.9 and 15.8-15.9 ppm, are substantially suppressed when these two proteins are complexed with the cognate transducer *pHtrII*, as shown in Figures 4B and 4F with reference to Figures 4A and 4E, respectively. This sort of the spectral change turns out to be less pronounced for A149S mutant, however (Figures 4C and 4D). As to the assignment of the above-mentioned peaks, we previously demonstrated that the peaks at 16.7-16.9 and 15.8-15.9 ppm were ascribed to the more flexible tip (Ala228, 234, 236 and 238) and rather static stem (Ala221) regions of the C-terminal  $\alpha$ -helix in the cytoplasmic side, respectively. This assignment is made possible on the basis of our recent comparative  $^{13}\text{C}$  NMR study on intact *ppR* and truncated *ppR* (1-220) (Kawamura et al., *Biochemistry*, manuscript in preparation) and also in analogy with the data of the similar  $^{13}\text{C}$  NMR studies on  $[3-^{13}\text{C}]\text{Ala}$ -labeled bR (23, 25, 27), as summarized in Table 1.

Obviously, such drastic intensity-changes by the complex-formation might be caused by an accompanied dynamics change at the flexible tip and (rather static) stem portions of the C-terminal  $\alpha$ -helical region from the fluctuation frequency in the order from  $10^8$  Hz and  $10^6$  Hz in the uncomplexed state to  $10^5$  Hz in the complexed state, respectively. This is a consequence of the peak-broadenings due to a failure of the proton decoupling, interfered with frequency of coherent proton decoupling and incoherent fluctuation frequency in the order of  $10^5$  Hz in the surface structure (21,27,31,35). Naturally, such a spectral change is more pronounced in the larger dynamics change in the flexible tip portion. It is further noted that the peaks in the loop region at 17.2 and 17.4 ppm, which cannot be usually observed in bR or *ppR*

incorporated as a monomer in lipid bilayers, emerge in the 2:2 complex of *ppR-pHtrII* (1-159) as a result of an “escape” from such interference leading to the peak-suppression(Figure 4 (B)).

This finding strongly indicates that the cytoplasmic C-terminal  $\alpha$ -helix in *ppR* and the cytoplasmic  $\alpha$ -helix (TM2) in *pHtrII*, protruding from the membrane surface, are also participated in the stability of the complex-formation with *pHtrII* (1-159), besides the role of the above-mentioned transmembrane  $\alpha$ -helices as revealed by the CP-MAS NMR experiments. In this connection, it appears that Ala149 or Val 149 for *ppR* and A149V mutant are stably located at the corner of the transmembrane  $\alpha$ -helix E in the vicinity of the E-F loop, although its direct evidence as to the mutant is unavailable at moment but might play an important role for the stabilization of the complex with *pHtrII*(1-159) in the cytoplasmic side.

## DISCUSSION

We found that the  $^{13}\text{C}$  DD-MAS NMR peak-intensities of the C-terminal  $\alpha$ -helix from  $[3-^{13}\text{C}]\text{Ala-ppR}$  and A149V are substantially reduced when they are complexed with the cognate transducer *pHtrII*(1-159) (Figures 4B and 4F), whereas those of  $[3-^{13}\text{C}]\text{Ala-A149S}$  are almost unchanged (Figure 4D). This is obviously caused by the characteristic dynamics change leading to reduced fluctuation frequency, in the surface structure including the C-terminal stem and tip portion of the  $\alpha$ -helix and the E-F loop of *ppR*, which is interfered with the proton decoupling frequency ( $10^5$  Hz). This finding suggests that mutual interaction between the two types of  $\alpha$ -helices, the C-terminal  $\alpha$ -helix of *ppR* and cytoplasmic  $\alpha$ -helix of *pHtrII* (1-159) (TM2) is responsible for the

stabilization of the complex as viewed from the surface structure. Indeed, we also demonstrated that the C-terminal  $\alpha$ -helix of *ppR* is a very important site to be able to interact with the cytoplasmic  $\alpha$ -helix of *pHtrII* (1-159) (Kawamura et al., *Biochemistry*, manuscript in preparation), although the surface structure of A149S mutant is not participated in the stabilization of the complex at the membrane surface. This means that the surface structure of the latter could be significantly modified to the extent that such a mutual interaction is geometrically unfavorable. Nevertheless, it should be pointed out that the *ppR-pHtrII* interaction in the transmembrane region remains unchanged among *ppR*, A149V and A149S as manifested from the similar  $^{13}\text{C}$  CP-MAS NMR spectra (Figure 2).

The three-dimensional structure of the *ppR-pHtrII* complex as viewed from the transmembrane region has been shown by x-ray diffraction study on crystalline sample (8) and EPR study on spin-labeled reconstituted preparation (41): the straight TM2 (C-terminal side) is oriented parallel to the helix G of the receptor, although the residues (115-159) in the cytoplasmic  $\alpha$ -helix of the truncated transducer (1-114) used is absent in the former (8). Therefore, it appears that the transmembrane  $\alpha$ -helix G of *ppR* is in direct contact with the TM2  $\alpha$ -helix of *pHtrII*(1-159) leading to stabilization of the surface structure. Therefore, it is likely that the E-F loop of *ppR* interacts with the membrane proximal region in *pHtrII*(1-159) (14) in an indirect manner, because its direct interaction with the transducer might be stereochemically unfavorable as viewed from the relative orientation of these moieties (8,41). It is probable, therefore, that the location of the hydrophobic Ala 149 (and also Val 149) at the corner of the helix E, linked to the hydrophilic E-F loop, is very important for the sake of maintaining the surface structure necessary for the mutual interaction between the receptor and

transducer. Indeed, Ala149 (and Val 149) in *ppR* is well conserved for the other archaeal retinal proteins (11). On the contrary, the helical structure at the position 149 might be less stable for Ser 149 at this corner in A149S mutant, especially at the interface between the hydrophobic and hydrophilic environment. In fact, it is known that Ala, Val, and Ser residues are strong  $\alpha$ -helix former,  $\alpha$ -former and indifferent for  $\alpha$ -helix, respectively (42). In addition to the change of stabilization in the corner of the helix E, the change of hydrophathy among Ala149, Val149 and Ser149 may be also responsible for surface dynamics (43). Therefore, the surface structure might be distorted to some extent from that of wild-type protein and is unfavorable for the stabilization of the complex as viewed from the cytoplasmic surface, although the strong hydrogen bond Y199<sup>*ppR*</sup>-N74<sup>*pHtrII*</sup>, and T189<sup>*ppR*</sup>-E43<sup>*pHtrII*</sup>, S62<sup>*pHtrII*</sup> in transmembrane region are conserved in *ppR* and these two kinds of mutants (5,9,12-15). This is the reason why the influence by the mutations is rather limited to the area of cytoplasmic side.

In contrast, it is also interesting to note that a single-mutation in the E-F loop results in significantly modified surface and dynamics structures in *bR* which also include the C-terminal  $\alpha$ -helix and the E-F loop, as manifested from the <sup>13</sup>C NMR spectra of A160G and A160V of *bR* mutants (corresponding to Ala149 in *ppR*) (25,29) (Table 1), by taking into account of the well-known structural homology between *ppR* and *bR*. It is, therefore, suggested that dynamics of the membrane surface residues including the E-F loop in the cytoplasmic side in *ppR* are strongly correlated with the manner of mutual interaction with *pHtrII* and its resulting biological function in relation to signal relay.

Finally, it is pointed out that site-directed <sup>13</sup>C NMR approach is a very valuable means to clarify a missing link between pictures by x-ray diffraction studies and

biological studies: a potential role of the mutual interactions between the cytoplasmic  $\alpha$ -helix in *ppR* and the cytoplasmic  $\alpha$ -helix in the C-terminus (TM2) in the cytoplasmic surface.

## **CONCLUSION**

It was revealed that dynamics of membrane surface residues in *ppR* complexed with *pHtrII* (1-159) were greatly changed among *ppR*, A149V and A149S mutants. Therefore, the surface structure near E-F loop of *ppR* plays dominant role to regulate membrane surface dynamics when *ppR* interacts with *pHtrII*(1-159) through direct interaction of the C-terminal  $\alpha$ -helix region in *ppR* interacts with the cytoplasmic  $\alpha$ -helical region of *pHtrII* (1-159). These interactions may correlate with the signal relay mechanism.

## **ACKNOWLEDGEMENTS**

The present work was supported by a Grant-in-Aid for Scientific Research on Priority Area (No. 17048010) from MEXT, Japan and for Scientific Research (No. 17370054) from JSPS, and by Research Grant-in-Aid from Magnetic Health Science Foundation. I. K. thanks young grant for “Research Aid Program for Ph. D. Candidates” on Yokohama National University.

## REFERENCES

1. Spudich, J. L. (1998) Variations on a molecular switch: transport and SENSORY signaling by archaeal rhodopsins, *Mol. Microbiol.* **28**, 1051-1058.
2. Kamo, N., K. Shimono, M. Iwamoto and Y. Sudo (2001) Photochemistry and photoinduced proton-transfer by *pharaonis* phoborhodopsin, *Biochemistry (Moscow)* **66**, 1277-1282.
3. Yang, C. S. and J. L. Spudich. (2001) Light-induced structural changes occur in the transmembrane helices of the *Natronobacterium pharaonis* HtrII transducer, *Biochemistry* **40**, 14207-14214.
4. Sudo, Y., M. Iwamoto, K. Shimono and N. Kamo (2001) *pharaonis* Phoborhodopsin binds to its cognate truncated transducer even in the presence of a detergent with a 1:1 stoichiometry, *Photochem. Photobiol.* **74**, 489-494.
5. Sudo, Y., H. Kandori and N. Kamo (2004) Molecular mechanism of protein-protein interaction of *pharaonis* phoborhodopsin/transducer and photo-signal transfer reaction by the complex, *Recent Res. Devel. Biophys.* **3**, 1-16.
6. Wegner, A. A., J. P. Klare, M. Engelhard and H. J. Steinhoff (2001) Structural insights into the early steps of receptor-transducer signal transfer in archaeal phototaxis, *EMBO J.* **20**, 5312-5319.
7. Luecke, H., B. Schobert, J. K. Lanyi, E. N. Spudich and J. L. Spudich (2001) Crystal structure of sensory rhodopsin II at 2.4 Angstroms: insight into color tuning and transducer interaction, *Science* **293**, 1499-1503.
8. Gordeliy, V. I., J. Labahn, R. Moukhametzianov, R. Efemov, J. Granzin, R. Schlesinger, G. Buldt, T. Savopoul, A. Scheldig, J. P. Klare and M. Engelhard (2002) Molecular basis of transmembrane signaling by sensory rhodopsin II-transducer

- complex, *Nature* **419**, 484-487.
9. Moukhametzianov, R., J. P. Klare, R. Efremov, C. Baeken, A. Goppner, J. Labahn, M. Engelhard, G. Büldt and V. I. Gordeliy (2006) Development of the signal in sensory rhodopsin and its transfer to the cognate transducer. *Nature* **440**, 115-119.
  10. Sudo, Y., M. Iwamoto, K. Shimono and N. Kamo (2002) Tyr-199 and charged residues of *pharaonis* phoborhodopsin are important for the interaction with its transducer, *Biophys. J.* **83**, 427-432.
  11. Ihara, K., T. Umemura, I. Katagiri, T. Kitajima-Ihara, Y. Sugiyama, Y. Kimura and Y. Mukohata (1999) Evolution of the archaeal rhodopsins: Evolution rate changes by gene duplication and functional differentiation, *J. Mol. Biol.* **285**, 163-174.
  12. Sudo, Y., M. Yamabi, S. Kato, C. Hasegawa, M. Iwamoto, K. Shimono and N. Kamo (2006) Importance of specific hydrogen bonds of archaeal rhodopsins for the binding to the transducer protein, *J. Mol. Biol.* **357**, 1274-1282.
  13. Sudo, Y., Y. Furutani, K. Shimono, N. Kamo and H. Kandori (2003) Hydrogen bonding alteration of Thr-204 in the complex between *pharaonis* phoborhodopsin and its transducer protein, *Biochemistry* **42**, 14166-14172.
  14. Sudo, Y., M. Yamabi, M. Iwamoto, K. Shimono and N. Kamo (2003) Interaction of *Natronobacterium pharaonis* phoborhodopsin (sensory rhodopsin II) with its cognate transducer probed by increase in the thermal stability. *Photochemistry and Photobiology* **78**, 511-516.
  15. Furutani, Y., K. Kamada, Y. Sudo, K. Shimono, N. Kamo and H. Kandori (2005) Structural changes of the complex between *pharaonis* phoborhodopsin and its cognate transducer upon formation of the M Photointermediate, *Biochemistry* **44**, 2909-2915.

16. Yang, C. S., O. Sineshchekov, E. N. Spudich and J. L. Spudich (2004) The cytoplasmic membrane-proximal domain of the HtrII transducer interacts with the E-F loop of photoactivated *Natronomonas pharaonis* sensory rhodopsin II, *J. Biol. Chem.* **279**, 42970-42976.
17. Hippler-Mreyen, S., J. P. Klare, A. A. Wegener, R. Seidel, C. Herrmann, G. Schmies, G. Nagel, E. Bamberg and M. Engelhard (2003) Probing the sensory rhodopsin II binding domain of its cognate transducer by calorimetry and electrophysiology, *J. Mol. Biol.* **330**, 1203-1213.
18. Chen, X. and J. L. Spudich (2004) Five residues in the HtrI transducer membrane-proximal domain close the cytoplasmic proton-conducting channel of sensory rhodopsin I, *J. Biol. Chem.* **279**, 42964-42969.
19. Saitô, H., S. Tuzi, M. Tanio and A. Naito (2002) Dynamic aspects of membrane proteins and membrane-associated peptides as revealed by  $^{13}\text{C}$  NMR: Lessons from bacteriorhodopsin as an *Intact* protein, *Annu. Rep. NMR Spectrosc.* **47**, 39-108.
- 20 Saitô, H., I. Ando and A. Naito (2006) *Solid state NMR spectroscopy for biopolymers: principles and applications*, Springer, Dordrecht, The Netherland
- 21 Saitô, H., Y. Kawase, A. Kira, K. Yamamoto, M. Tanio, S. Yamaguchi, S. Tuzi and A. Naito (2007) Surface and dynamic structures of bacteriorhodopsin in a 2D crystal, a distorted or disrupted lattice, as revealed by site-directed solid-state  $^{13}\text{C}$  NMR, *Photochem. Photobiol.* in press. (This issue)
22. Watts, A. (1998) Solid-state NMR approaches for studying the interaction of peptides and proteins with membranes, *Biochim. Biophys. Acta.* **1376**, 297-318.
23. Saitô, H., J. Mikami, S. Yamaguchi, M. Tanio, A. Kira, T. Arakawa, K. Yamamoto and S. Tuzi (2004) Site-directed  $^{13}\text{C}$  solid-state NMR studies on membrane proteins:

- strategy and goals toward revealing conformation and dynamics as illustrated for bacteriorhodopsin labeled with [1-<sup>13</sup>C]amino acid residues, *Magn. Reson. Chem.* **42**, 218-230.
24. Tuzi, S., J. Hasegawa, R. Kawaminami, A. Naito and H. Saitô (2001) Regio-selective detection of dynamic structure of transmembrane  $\alpha$ -helices as revealed from <sup>13</sup>C NMR spectra of [3-<sup>13</sup>C]Ala-labeled bacteriorhodopsin in the presence of Mn<sup>2+</sup> ion, *Biophys. J.* **81**, 425-434.
25. Yamaguchi, S., K. Yonebayashi, H. Konishi, S. Tuzi, A. Naito, J. K. Lanyi, R. Needleman and H. Saitô (2001) Cytoplasmic surface structure of bacteriorhodopsin consisting of interhelical loops and C-terminal  $\alpha$  helix, modified by a variety of environmental factors as studied by <sup>13</sup>C NMR, *Eur. J. Biochem.* **268**, 2218-2228.
26. Barré, P., S. Yamaguchi, H. Saitô and D. Huster (2003) Backbone dynamics of bacteriorhodopsin as studied by <sup>13</sup>C solid-state NMR spectroscopy, *Eur. Biophys. J.* **32**, 578-584.
27. Saitô, H., S. Tuzi, S. Yamaguchi, M. Tanio and A. Naito (2000) Conformation and backbone dynamics of bacteriorhodopsin revealed by <sup>13</sup>C-NMR., *Biochem. Biophys. Acta.* **1460**, 39-48.
28. Saitô, H., S. Yamaguchi, K. Ogawa, S. Tuzi, M. Márquez, C. Sanz and E. Padrós (2004) Glutamic acid residues of bacteriorhodopsin at the extracellular surface as determinants for conformation and dynamics as revealed by site-directed solid-state <sup>13</sup>C NMR, *Biophys. J.* **86**, 1673-1681.
29. Yonebayashi, K., S. Yamaguchi, S. Tuzi and H. Saitô (2003) Cytoplasmic surface structures of bacteriorhodopsin modified by site-directed mutations and cation binding as revealed by <sup>13</sup>C NMR, *Eur. Biophys. J.* **32**, 1-11.

30. Arakawa, T., K. Shimono, S. Yamaguchi, S. Tuzi, Y. Sudo, N. Kamo and H. Saitô (2003) Dynamic structure of *pharaonis* phoborhodopsin (sensory rhodopsin II) and complex with a cognate truncated transducer as revealed by site-directed  $^{13}\text{C}$  solid-state NMR, *FEBS Lett.* **536**, 237-240.
31. Yamaguchi, S., K. Shimono, Y. Sudo, S. Tuzi, A. Naito, N. Kamo and H. Saitô (2004) Conformation and dynamics of the [3- $^{13}\text{C}$ ]Ala-, [1- $^{13}\text{C}$ ]Val-labeled truncated *pharaonis* transducer, pHtrII(1-159) as revealed by site-directed  $^{13}\text{C}$  solid-state NMR: Changes due to association with phoborhodopsin (sensory rhodopsin II), *Biophys. J.* **86**, 3131-3140.
32. Shimono, K., M. Iwamoto, M. Sumi and N. Kamo (1997) Functional expression of *pharaonis* phoborhodopsin in *Escherichia coli*, *FEBS Lett.* **420**, 54-56
33. Kandori, H., K. Shimono, Y. Sudo, M. Iwamoto, Y. Shichida and N. Kamo (2001) Structural changes of *pharaonis* phoborhodopsin upon photoisomerization of the retinal chromophore: Infrared spectral composition with bacteriorhodopsin, *Biochemistry* **40**, 9238-9246.
34. Bennet, A. W., C. M. Rienstra, M. Augar, K. V. Lakshmi and R. G. Griffin (1995) Heteronuclear decoupling in rotating solids, *J. Chem. Phys.* **103**, 6951-6958.
35. Rothwell, W. P. and J. S. Waugh (1981) Transverse relaxation of dipolar coupled spin systems under rf irradiation: detection motions in solid, *J. Chem. Phys.* **75**, 2721-2732.
36. Naito, A., A. Fukutani, M. Uitdehaag, S. Tuzi and H. Saitô (1998) Backbone dynamics of polycrystalline peptides studied by measurements of  $^{15}\text{N}$  NMR lineshapes and  $^{13}\text{C}$  transverse relaxation times, *J. Mol. Struct.* **441**, 231-241.
37. Krimm, S. and A. M. Dwivedi (1982) Infrared spectrum of the purple membrane:

- clue to a proton conduction mechanism?, *Science*. **216**, 407-408.
38. Saitô, H. and I. Ando (1989) High-resolution solid-state NMR studies of synthetic and biological macromolecules, *Annu. Rep. NMR spectrosc.* **21**, 209-290.
- 39 Howarth, O. W. and D. M. J. Lilley (1978) Carbon-13 NMR of peptides and proteins. *Prog. NMR Spectrosc.*, **12**, 1-40
- 40 Tuzi, S., S. Yamaguchi, A. Naito, R. Needleman, J. K. Lanyi and H. Saitô (1996) Conformation and dynamics of [3-<sup>13</sup>C]Ala-labeled bacteriorhodopsin and bacterioopsin, induced by interaction with retinal and its analogs, as studied by <sup>13</sup>C nuclear magnetic resonance. *Biochemistry*, **35**, 7520-75227
- 41 Wegener, A.-W., J. P. Klare, M. Engelhard and H.-J. Steinhoff (2001) Structural insights into the early steps of receptor-transducer signal transfer in archaeal phototaxis. *EMBO J.*, **20**, 5312-5319.
- 42 Chou, P. Y. and G. D. Fasman (1974) Conformational parameters for amino acids in helical,  $\beta$ -sheet, and random coil regions calculated from proteins. *Biochemistry*, **13**, 222-245
- 43 Kyte, J. and R. F. Doolittle (1982) A simple method for displaying the hydrophobic character of a protein. *J. Mol. Biol.*, **157**, 105-132.

Table 1.  $^{13}\text{C}$  chemical shifts of [3- $^{13}\text{C}$ ]Ala-labeled *ppR* with reference to those of the corresponding residues in *bR*. (ppm from TMS)

Residues	Location	$\delta_{\text{iso}}$ (ppm)	Assignment based on mutants
<i>ppR</i>			A149V,A14S
Ala149	Helix E	15.9 <sup>a</sup>	A149S- <i>pHtrII</i> (1-159), A149V- <i>pHtrII</i> (1-159)
Ala221	C-terminal $\alpha$ -helix (stem)	15.8 <sup>a</sup>	<i>ppR</i> (1-220)
Ala228, 234, 236, 238	C-terminal $\alpha$ -helix (tip)	16.7-16.9 <sup>a</sup>	<i>ppR</i> (1-220)
<i>bR</i>			
Ala160	E-F loop	17.38 <sup>b</sup>	A160G
Ala228,233	C-terminal $\alpha$ -helix	15.91 <sup>b</sup>	Cleavaged C-terminal
Ala240,244-246	C-terminal random coil	16.88 <sup>b</sup>	Cleavaged C-terminal

<sup>a</sup> The measurements of *ppR* were performed at 20 °C with a *ppR*-to-egg PC molar ratio of 1:50 (I. Kawamura et al, *Biochemistry*, in preparation).

<sup>b</sup> Data from [23,25].

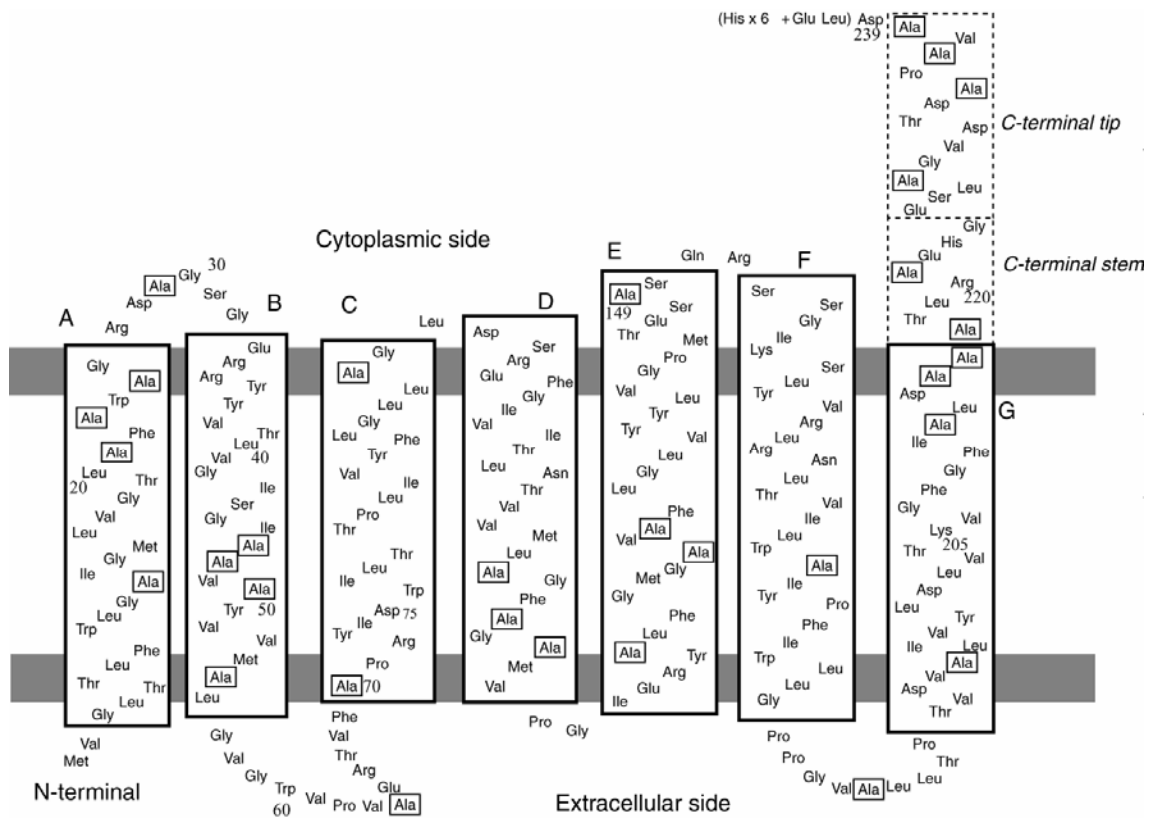
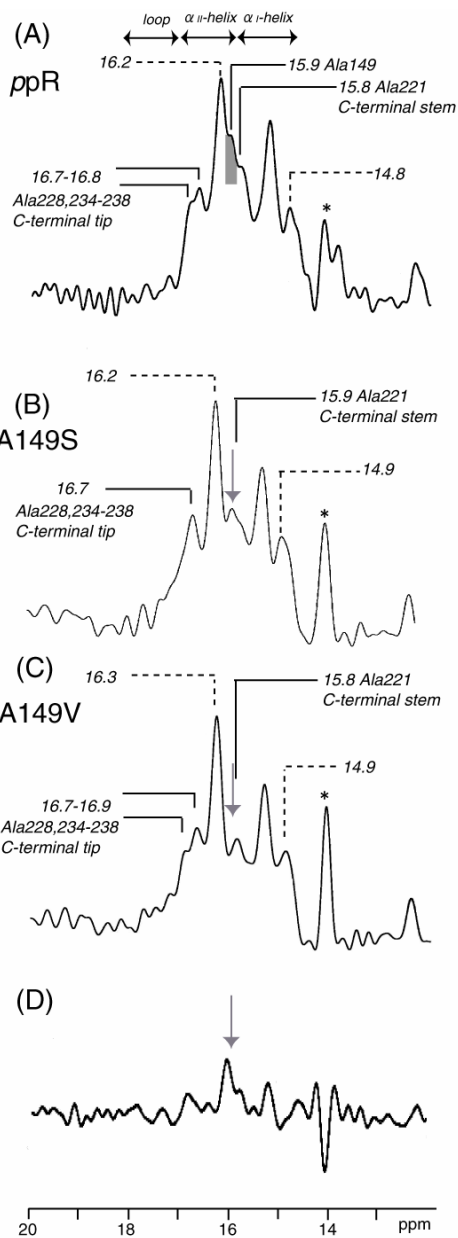


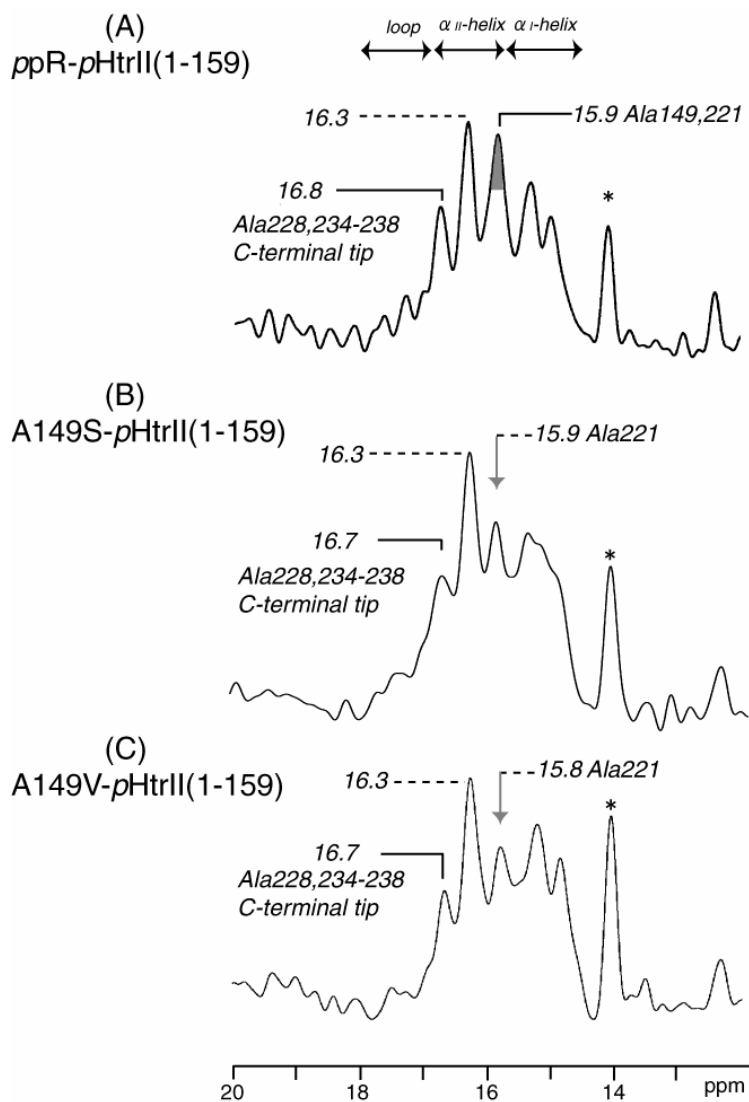
Figure 1  
Kawamura et al.

Figure 1: A schematic representation of the secondary structures in ppR based on crystallographic structures reported by H. Luecke et al. (ppR: PDB code 1JGJ) and V. I. Gordeliy et al. (ppR-pHtrII(1-114): PDB code 1H2S) The surface areas of the lipid bilayer are represented by gray bands.



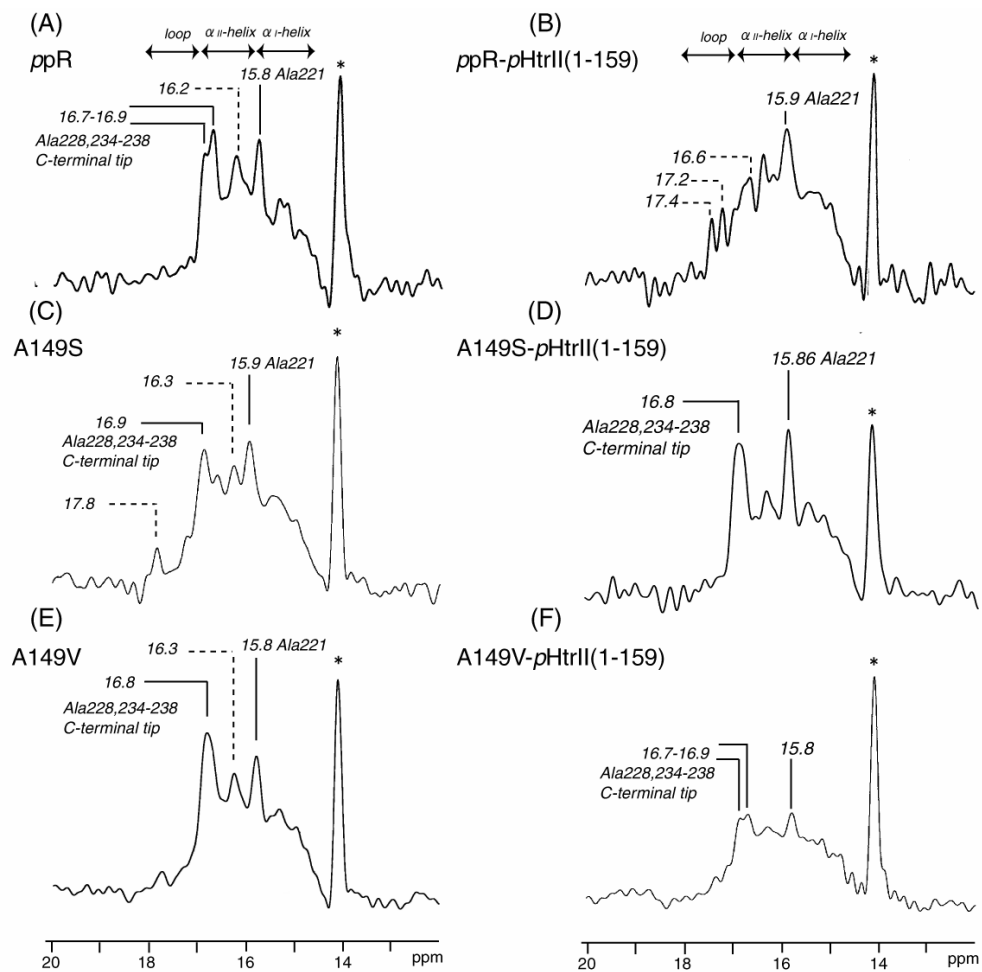
**Figure 2**  
*Kawamura et al.*

Figure 2:  $^{13}\text{C}$  CP-MAS NMR spectra of uncomplexed  $[3-^{13}\text{C}]$ Ala-labeled ppR(A), A149S(B) and A149V(C) alone, reconstituted in egg PC bilayer.  $^{13}\text{C}$  NMR signal at 15.9 ppm corresponding to Ala149 in ppR is shown in the gray (A) and arrows (B and C). The resonance peak at 14.1 ppm is ascribed to methyl carbon peak of egg PC as shown as asterisk. Difference spectrum between (A) and (B) is shown in (D).



**Figure 3**  
**Kawamura et al.**

Figure 3:  $^{13}\text{C}$  CP-MAS NMR spectra of  $[3-^{13}\text{C}]$ Ala-labeled  $ppR$  (A),  $A149S$  (B) and  $A149V$  (C) complexed with  $pHtrII(1-159)$ , reconstituted in egg PC bilayer.  $^{13}\text{C}$  NMR signal from Ala149 in the vicinity of EF loop in  $ppR$  is shown in the gray (A) and arrows (B and C). The resonance peak at 14.1 ppm is the methyl carbon peak of egg PC as shown as asterisk.



**Figure 4**  
*Kawamura et al.*

Figure 4:  $^{13}\text{C}$  DD-MAS NMR spectra of uncomplexed  $[3\text{-}^{13}\text{C}]\text{Ala}$ -labeled *ppR* (A), A149S (C) and A149V (E) (left panel) and those complexed with *pHtrII*(1-159) (right panel). And those of *ppR* (B), A149S(D) and A149V(F) complexed with *pHtrII*(1-159) reconstituted in egg PC bilayer (right panel)

